Acta Oceanol. Sin., 2016, Vol. 35, No. 11, P. 52–58
DOI: 10.1007/s13131-016-0847-4
http://www.hyxb.org.cn
E-mail: hyxbe@263.net

Evaluating a satellite-based sea surface temperature by shipboard survey in the Northwest Indian Ocean

YANG Guang[1, 2], HE Hailun[2]*, WANG Yuan[2], HAN Xiqiu[3], WANG Yejian[3]

[1] Ocean College, Zhejiang University, Zhoushan 316021, China

[2] State Key Laboratory of Satellite Ocean Environment Dynamics, Second Institute of Oceanography, State Oceanic Administration, Hangzhou 310012, China

[3] Key Laboratory of Submarine Geosciences, Second Institute of Oceanography, State Oceanic Administration, Hangzhou 310012, China

Received 26 October 2015; accepted 27 January 2016

Abstract

A summer-time shipboard meteorological survey is described in the Northwest Indian Ocean. Shipboard observations are used to evaluate a satellite-based sea surface temperature (SST), and then find the main factors that are highly correlated with errors. Two satellite data, the first is remote sensing product of a microwave, which is a Tropical Rainfall Measuring Mission Microwave Imager (TMI), and the second is merged data from the microwave and infrared satellite as well as drifter observations, which is Operational Sea Surface Temperature and Sea Ice Analysis (OSTIA). The results reveal that the daily mean SST of merged data has much lower bias and root mean square error as compared with that from microwave products. Therefore the results support the necessary of the merging infrared and drifter SST with a microwave satellite for improving the quality of the SST. Furthermore, the correlation coefficient between an SST error and meteorological parameters, which include a wind speed, an air temperature, a relative humidity, an air pressure, and a visibility. The results show that the wind speed has the largest correlation coefficient with the TMI SST error. However, the air temperature is the most important factor to the OSTIA SST error. Meanwhile, the relative humidity shows the high correlation with the SST error for the OSTIA product.

Key words: shipboard survey, sea surface temperature, Northwest Indian Ocean, Tropical Rainfall Measuring Mission Microwave Imager, Operational Sea Surface Temperature and Sea Ice Analysis

Citation: Yang Guang, He Hailun, Wang Yuan, Han Xiqiu, Wang Yejian. 2016. Evaluating a satellite-based sea surface temperature byshipboard survey in the Northwest Indian Ocean. Acta Oceanologica Sinica, 35(11): 52–58, doi: 10.1007/s13131-016-0847-4

1 Introduction

The sea surface temperature (SST) represents the thermostate of the near-surface ocean, controls the air-sea temperature difference and then determines the air-sea turbulent heat flux. Therefore, the SST is very important parameter in forcing both atmospheric and oceanic general circulation models (GCM), and it is the main exchange parameter in the coupled atmosphere and ocean GCM (Hu et al., 2013). As a most important interannual signal in the tropical Pacific, the El Niño/La Niña-Southern Oscillation (ENSO) is usually defined by an SST-based index (Lian et al., 2014; Wu et al., 2013, 2016; Chen et al., 2015). Also, the warm SST is necessary in the generation of a tropical cyclone. On the other hand, the spatial distributions of the global and regional SST show the important information of an ocean dynamics. An SST front is always accompanied with a geostrophic current (Liu et al., 2014, 2016); the SST is also used in detecting a mesoscale eddy (Dong et al., 2011). Hence, high quality SST data are necessary for multiscale processes in the atmosphere and the ocean and their coupled system (Donlon et al., 2009).

Satellite-based remote sensing is the main methodology to obtain the continuous global SST, however, the calibration of satellite SST by observation is the main processing of satellite images, and the quality of the satellite SST is always restricted by the regional observation capability. The satellite-based SST always has good performance in the well observation ocean. The comparison between the satellite SST and the *in situ* measurements has been conducted on the global ocean or local regions (Gentemann, 2014; O'Carroll et al., 2008, 2012; Williams et al., 2014). And the results show a good consistency between the satellite SST and the *in situ* SST in most areas. However, the error of the satellite SST product in the poor observation ocean is still significant. For example, Williams et al. (2014) have shown that the mean error for an Advanced Very High Resolution Radiometer (AVHRR) in Patagonia, Argentina is as large as 1.64 during the period of 2005–2009.

The Northwest Indian Ocean (NWIO) Basin is small but contains a diversity of the ocean dynamics caused by the seasonally reversing of wind (Burkill et al., 1993). Therefore, a collection of

Foundation item: China Ocean Mineral Resources Research and Development Association Project under contract No. DY125-12-R-03; the National Natural Science Foundation of China under contract Nos 41476021 and 41321004; the Scientific Research Fund of Second Institute of Oceanography, State Oceanic Administration China under contract No. JT1205.

*Corresponding author, E-mail: hailun@sio.org.cn

high accuracy and resolution SST satellite data become especially important for the research on the NWIO region. Many validation studies of the satellite-derived SST have been carried out in the tropical Indian Ocean (Senan et al., 2001; Parekh et al., 2007; Udaya et al., 2009), but the validation of the SST has rarely been focused on the NWIO region, and the present work is mainly motivated by this.

It is noted that many factors affect the accuracy of the satellite SST, including orbit and sensor stability, and variations and types of clouds, water vapor, aerosol concentrations and wind in the atmosphere (Reynolds, 1993; Wentz et al., 2000; Gentemann et al., 2004; Rapp et al., 2008). Park et al. (2011) have reported that the errors of the satellite SST have dependency on the moisture amount in the atmosphere, and the errors seemed to be underestimated in somewhat dry condition, and tended to be overestimated in a moist condition. Qiu et al. (2009) have examined the relationship between the wind speeds and the errors between the satellite SST and the shipboard SST. The results indicate that, the errors decrease with the wind speed when it keeps below 6 m/s, but shows less dependence on it for stronger wind. The analysis of dependence of the SST error on the meteorological parameters therefore shows a valuable reference to the further improvement of the satellite SST, and this is the second reason for performing present work.

We consider two widely used satellite data, the first is the Tropical Rainfall Measuring Mission Microwave Imager (TMI), and the other is the Operational Sea Surface Temperature and Sea Ice Analysis (OSTIA). The TMI SST was the first satellite microwave SST available and has proven to be of great value to many research areas. Compared with the infrared SST, the microwave SST has longer period of time, and better coverage in the open oceans. However, the spatial resolution of the microwave SST is not as good as the infrared SST (Reynolds et al., 2010). Thus, the effectively merging of the microwave SST and the infrared SST can therefore take the advantages of both data set but avoid their disadvantages. The OSTIA is a merged SST, which is owed to both advantages of cloud-free and high-resolution.

Our study in this paper is divided into two parts, one evaluates the satellite-derived SST using the shipboard observation, and the other is to find out the main factors that highly correlated with the SST errors. This work is organized as follows: Section 2 describes the data sources used in this study; a processing method are introduced in Section 3, the results are presented in Section 4; and Sections 5 and 6 are devoted to discussion and conclusions respectively.

2 Data

2.1 *Shipboard data*

A campaign is implemented by Chinese R/V *Lisiguang* for the 24th China Ocean Mineral Resources Research and Development Association (COMRA) cruise. The mission of the 24th COMRA cruise was to provide multidisciplinary surveys on the Carlsberg Ridge in the NWIO. The Carlsberg Ridge is a part of the Mid-Indian Ridge and traversing from the Rodrigues Trip junction to the Gulf of Aden, trending nearly from the Northwest to southeast. The depth of the Carlsberg Ridge is between about 1 800 m and 3 600 m. The intensive period of observation of the campaign is between May 10 and June 4 in 2012. Our shipboard survey is conducted back and forth continuously on the Carlsberg Ridge (Fig. 1).

The atmospheric parameters include the wind speed, the wind direction, the air temperature, the relative humidity, the air pressure and the visibility, and the ocean parameter SST is also obtained simultaneously. The details of meteorological sensors deployed on the 24th COMRA are listed in Table 1. The meteorological parameters are measured every hour. Among all the sensors, the infrared SST sensor was mounted at a level of 3 m above the mean sea level. It is noted that our SST sensors detected the skin SST, which made it more comparable with the satellite-retrieved product.

Figure 2 shows the time series of the meteorological paramet-

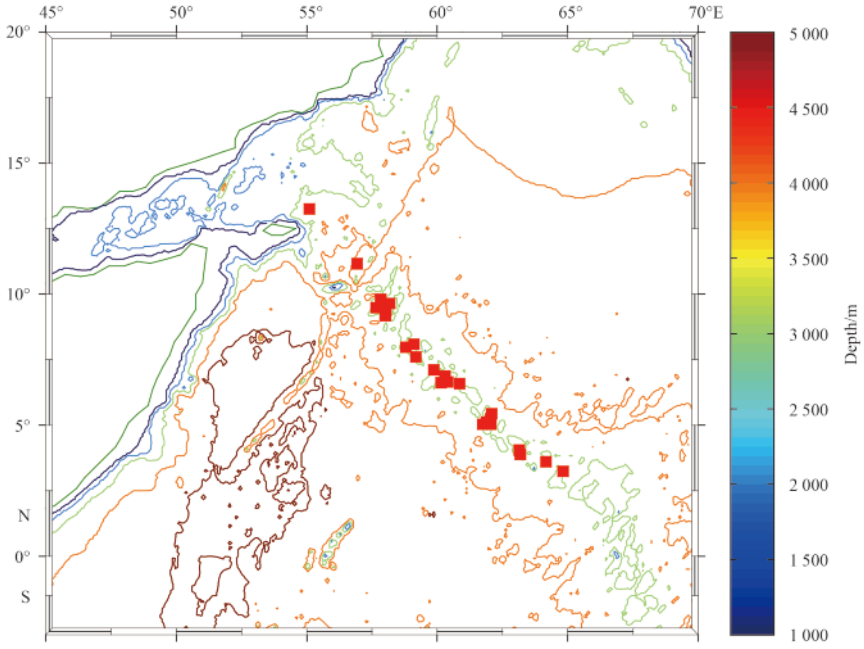

Fig. 1. Bathymetry of research area. Bathymetry data are extracted from ETOPO-5 min. The red squares are the daily mean locations of ship in the present study.

Table 1. Meteorological instrumentation deployed during COMRA 24th cruise

Sensor	Parameter	Range	Accuracy	Altitude/m
Three-cups wind vane	wind speed	0–65 m/s	±0.5 m/s	14
	wind direction	0°–360°	±6°	14
Infrared Temp. sensor 4000.3zl	SST	–3–60°C	±0.5°C	3
Barometer Setra278	air pressure	850–1 050 hPa	±1 hPa	13
Humidity and temp. sensor HMP45	air temperature	–40–60°C	±0.5°C	13
	relative humidity	0%–100%	±5%	13
Visibility sensor PWD20	visibility	10–20 000 m	±15%	14

ers. The SST variation shows a clear diurnal signal. The wind speed variation contains a high-frequency signal, and the maximum wind speed keeps below 12 m/s, which reveals that the survey is implemented under a moderate wind condition. The wind speeds during the first half period of survey are generally weaker than those during the other half time period. The temporal asymmetry on the visibility is also observed that, the visibility during the first half period is better than that in the other half time period. Meanwhile, a bad visibility condition is always accompanied with a relative high wind conditions. The air pressure varies between 100.7 and 101.3 kPa, and there are always two peaks per day, which reveal the subdiurnal variance on the signal. In contrast to the SST, the variances of the relative humidity and the air temperature are not obvious. The mean values of the relative humidity and the air temperature are 66.6% and 29.4°C, respectively, with the corresponding variances being 16.5% and 0.9°C respectively.

2.2 *TMI SST*

The TMI SSTs (Version 7.1 are used here) are provided by remote sensing systems, which include daily data (separated into ascending and descending orbit segments), three-day mean data, weekly and monthly data. The TMI SST covers a global region with valid data extending from 40°S to 40°N at a pixel resolution of 0.25°(≈25 km).

2.3 *OSTIA SST*

The OSTIA analysis is a merged, gridded, and gap-free SST data sets. The OSTIA system is one of the data process systems provided by the Met Office in the United Kingdom, and it is a persistence-based multiscale optimal interpolation system (Stark et al., 2007), that uses data from a combination of infrared and mi-

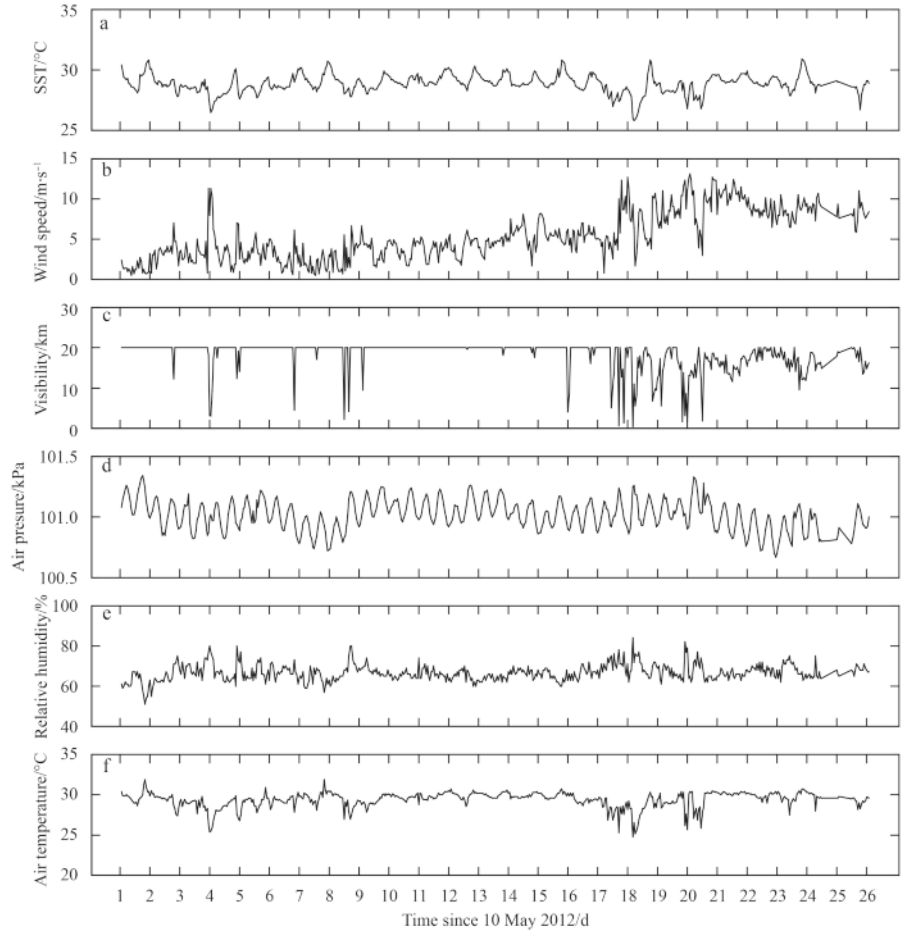

Fig. 2. Time series of meteorological parameters.

crowave satellites as well as *in situ* observations. The infrared satellite data used as system input data include AVHRR data products, Meteosat Second Generation Spinning Enhanced Visible and infrared radiometer data products, and ENVISAT Advanced Along-track Scanning Radiometer data products; the microwave satellite data are Aqua Advanced Microwave Scanning Radiometer for EoS, and Tropical Rainfall Mapping Mission TMI data products; and *in situ* data contain observations from ships, drifting and moored buoys reported on the Global Telecommunications System (Donlon et al., 2012). Meanwhile, the OSTIA SST has the global coverage, and its spatial resolution is 6.5 km.

3 Methodology

In order to obtain daily mean SST from a shipboard observation, we do some quality control on the source data, that is, the daily moving distance of ship should be lower than a threshold, which is defined as 300 km in the present study. The threshold definition reveals a balance between the data accuracy and the data number, on the sensing of that the daily averaged data would contain too much noise if we chosen too large distance threshold, otherwise, the number of sampling data would be too much small. Meanwhile the 300 km is about 3° in the longitude-latitude grid, which represents the typical horizontal resolutions in the modern ocean study. Figure 3 shows the daily moving distance of ship. Most daily moving distances are smaller than 300 km, and there are 18 good data after the quality control. It is worthy noted that the TMI satellite measures a skin surface temperature of about 0.01m, and the OSTIA chooses the depth of 0.2–1.0 m (Donlon et al., 2012; Senan et al., 2001). The SST difference introduced by the two depth is approximately 0.17°C (Donlon et al., 2002, 2012), which is supposed not significant in the present study.

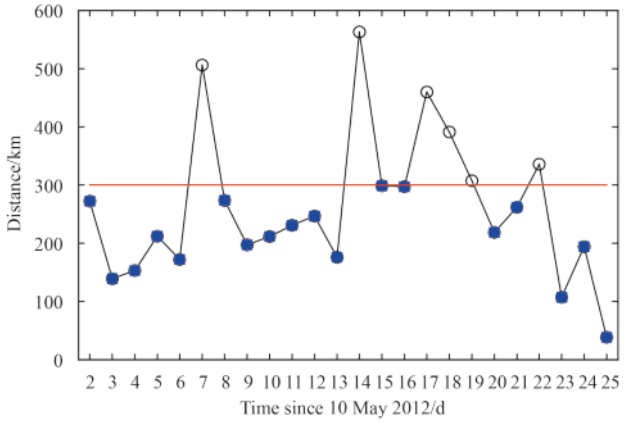

Fig. 3. The daily moving distance of ship.

The TMI SST image matches the nearest pixel to the observational locations. Figure 4 shows the results of matching between the shipboard SST and the TMI SST. It is observed that the TMI SST has the possibility of missing data at a given day. There are 15 daily mean shipboard SSTs available after matches with the TMI SST. It is also noted that 18 daily mean shipboard SSTs are selected for comparison with the OSTIA SST (figure is not shown here).

The satellite-derived SST is evaluated by four statistical indices in our study. The statistical indices include a correlation coefficient (CC, c_c), mean bias (MB, b_m), standard deviation (SD, d_s) and a root mean square error (RMSE, e_{rms}), and the indices are formulated as

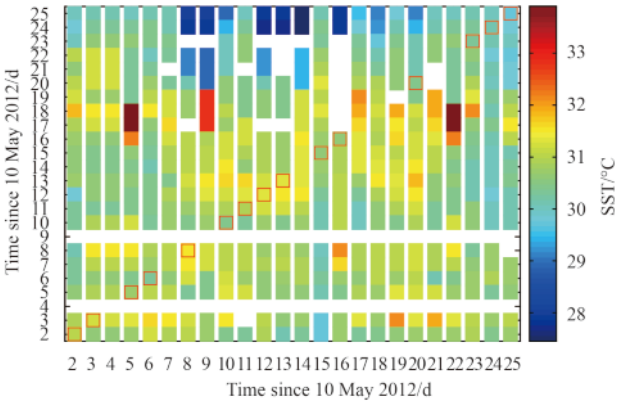

Fig. 4. The daily mean TMI SST at shipboard location. The red squares denote the matching between the shipboard observations and the TMI satellite data. The daily mean TMI SST is obtained by daily averaging the two data of descending and ascending from the daily TMI product.

$$CC = \frac{N\sum_{i=1}^{N} x_i y_i - \sum_{i=1}^{N} x_i . \sum_{i=1}^{N} y_i}{\sqrt{N\sum_{i=1}^{N} x_i^2 - \left(\sum_{i=1}^{N} x_i\right)^2} \cdot \sqrt{N\sum_{i=1}^{N} y_i^2 - \left(\sum_{i=1}^{N} y_i\right)^2}}, \quad (1)$$

$$MB = \frac{\sum_{i=1}^{N}(x_i - y_i)}{N}, \quad (2)$$

$$SD = \sqrt{\frac{\sum_{i=1}^{N}(MB - \overline{MB})^2}{N}}, \quad (3)$$

$$RMSE = \sqrt{\frac{\sum_{i=1}^{N}(x_i - y_i)^2}{N}}, \quad (4)$$

where x_i and y_i are the samples of two data sets.

4 Results

4.1 *Validation of TMI SST and OSTIA SST with shipboard SST*

We present the comparison between the satellite-retrieved data and the shipboard observations in Fig. 5. The TMI SST is obviously higher than the other two data sets. The shipboard SST is lower than the OSTIA SST both on the early and later of the survey, but they are almost consistent on the middle of the survey. The shipboard SST covered a temperature range between 28.12°C and 29.33°C, while the TMI SST is a higher value range between 30.15°C and 31.50°C, and the OSTIA SST has a moderate temperature range between 28.93°C and 30.27°C.

Figure 6 shows the scatter plot of the satellite-based SST and the shipboard SST. As also noted in the time series of the SST (Fig. 5), the TMI SST in Fig. 6a is significantly larger than the shipboard data. From Fig. 6b, it is clear that most of the matching are above the black line, but there still a few matchings under the black line, which means that the shipboard SST is larger than the OSTIA SST for some matchings. The CC between the TMI and shipboard SSTs is 0.39, the corresponding value between the OSTIA and shipboard SSTs is –0.38. The MB plus or minus the SD

(the RMSE) of the TMI SST is (1.80±0.45)°C (1.85°C). While the MB plus or minus the SD (the RMSE) of the OSTIA SST is (0.73±0.68)°C (1.00°C). The MB indicated a large overestimation of the TMI data in respect to observational records. The bias is improved by 1.07°C for the OSTIA against the TMI. It is also noted the RMSE of the OSTIA is 0.85°C smaller than that of the TMI.

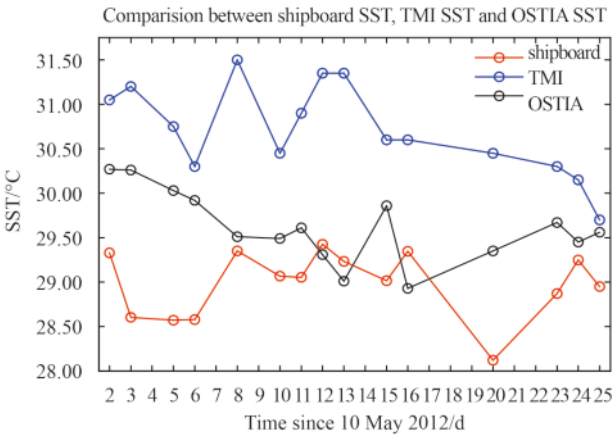

Fig. 5. Time series of the SST from the shipboard observations, the TMI and the OSTIA.

4.2 *Factors affecting satellite-based SST errors*

Figure 7 shows the dependence of the TMI SST errors on the meteorological parameters, which include the wind speed, the visibility, the air pressure, the relative humidity and the air temperature. The results indicate that the SST errors are mainly dependent on the wind speed and the air temperature. The CC between the wind speed and the error is –0.36, and Fig. 7a clearly indicates that the error between the TMI SST and the shipboard SST become larger when the wind speed decrease. Figure 7e shows a negative CC (–0.55) between the air temperature, and the absolute value of CC is even higher than wind speed. The CCs of the SST errors with visibility, air temperature and relative humidity are lower than those with wind speed and air temperature, and the CCs keep below 0.20.

The dependences of the OSTIA SST errors on the meteorological parameters are shown in Fig. 8. It is observed that the most

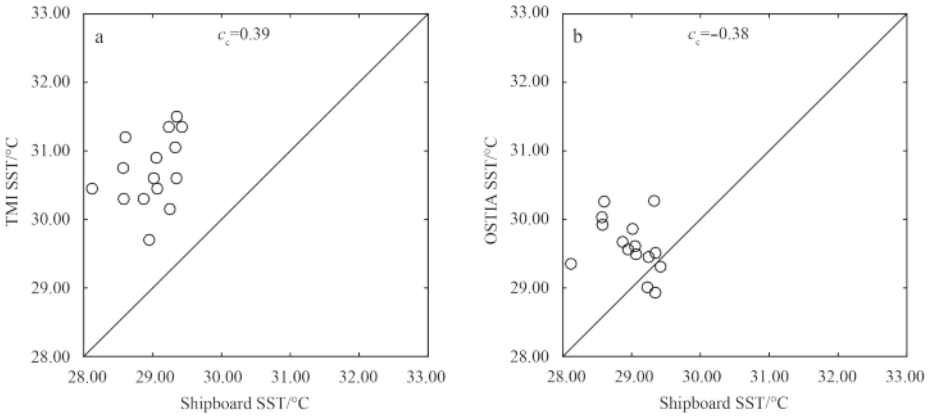

Fig. 6. Scatter diagrams of the TMI SST versus the shipboard SST (a), and the OSTIA SST versus the shipboard SST (b). The black line indicates a perfect fitting line.

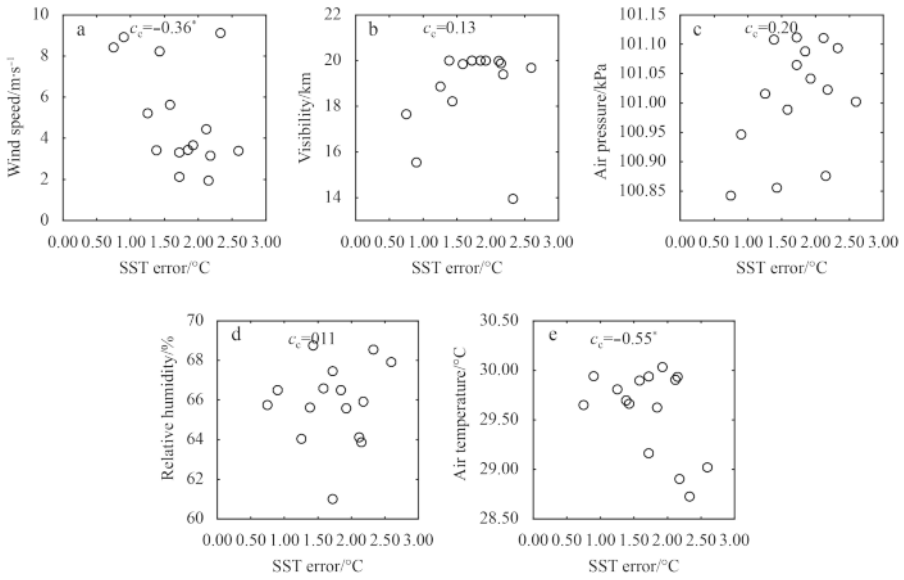

Fig. 7. Dependences of the TMI SST errors on the wind speed (a), the visibility (b), the air pressure (c), the relative humidity (d) and the air temperature (e). The asterisks denote the statistical significance at the 90% level.

important parameter affecting the OSTIA SST errors is the air temperature (Fig. 8e). The CC between the air temperatures and the OSTIA SST errors shows the highest absolute value as –0.80. The secondary large CC is given by the relative humidity (Fig. 8d), and the value is 0.56. The CCs for other factors are about 0.10 except air pressure, which is only 0.02.

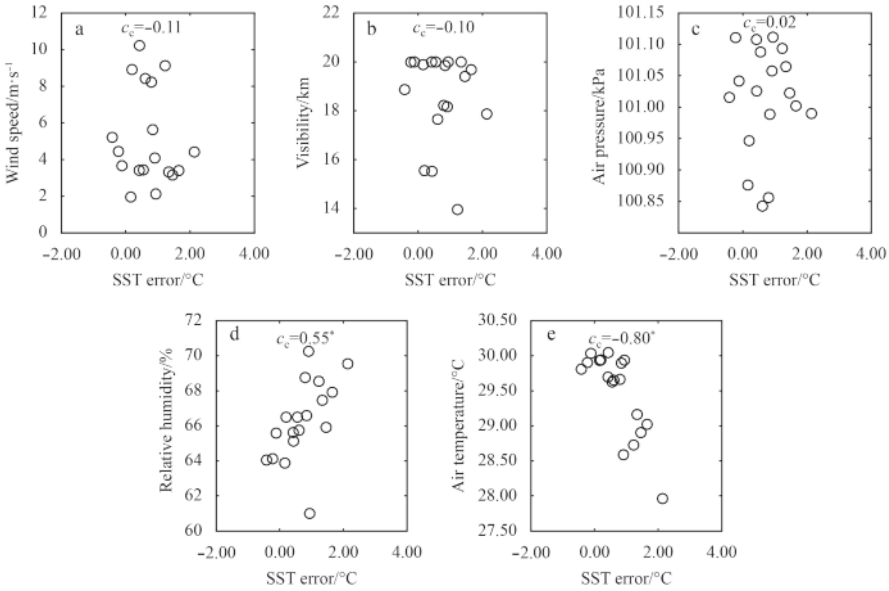

Fig. 8. Dependences of the OSTIA SST error on the wind speed (a), the visibility (b), the air pressure (c), the relative humidity (d) and the air temperature (e). The asterisks denote the statistical significance at the 90% level.

5 Discussion

The mean bias of the TMI SST is as large as 1.8°C, and this significant SST bias was also observed in the existed study. The *in situ* SST measurement also shows generally 1.50°C difference lower than the TMI SST during the tropical cyclone stage (Bell et al., 2012). Then the RMSE of the OSTIA SST is about 1.00°C, which is slightly larger than that produced by the data supporter (Stark et al., 2007; Donlon et al., 2012), where the RMSE of the OSTIA SST is 0.70°C and 0.57°C, by Stark et al. (2007) and Donlon et al. (2012) respectively. The accuracy of the OSTIA SST is better than the TMI SST when both mean bias and the RMSE were considered. Although our third-party data did not get involved in the merging processing, our evaluation also supports the advantage of merging data.

In terms of the TMI SST, the bias is so large that it may come from complex reasons. There is at least one reason that can be mentioned as the diurnal variation signal of the TMI SST has not been filtered out. The temporal resolution of the TMI SST is too low to describe the diurnal variation correctly, for only two data per day. This may lead to a large deviation for the daily SST from the real data. In addition, the wind speed dependence of the TMI SST error is consistent with the previous results (Qiu et al., 2009; Park et al., 2011).

The bias of the OSTIA SST may be come from inaccuracy or poorly specified single sensor error statistics of the input satellite data (Stark et al., 2007). The dependence of the OSTIA SST bias on the relative humidity is probably determined by the characteristics of an infrared satellite. The existed studies have reported that the infrared SST has dependency on the moisture amount in the atmosphere (Walton, 1988; Park et al., 1994, 1999). And the reason for the dependence may be explained with the fact that moist air generally occurs over warm seas, so that the atmospheric relative humidity increases with the SST. Therefore, the post-process of the OSTIA is suggested to consider more information of the relative humidity.

Sometimes the TMI can be the only source that delivery instantaneous SST, such as in areas or periods that other satellites cannot cover (Gentemann et al., 2004). Therefore, we evaluate the instantaneous SST interpolated from the daily TMI product, as shown in Fig. 9. It is observed that the instantaneous TMI SST overestimates the observed SST, and the mean bias is 1.94, which is comparable with the error of the TMI daily SST evaluation. However, the CC is only as poor as 0.05, this may be because the interpolation caused the missing of the diurnal variation of the SST. The instantaneous TMI SST is suggested to be used carefully in some occasions.

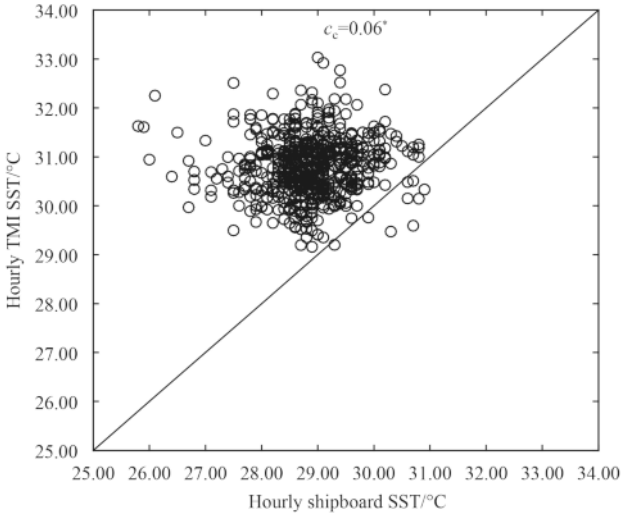

Fig. 9. Dependences of the OSTIA SST error on the wind speed (a), the visibility (b), the air pressure (c), the relative humidity (d) and the air temperature (e). The asterisks denote the statistical significance at the 90% level.

6 Conclusions

We implemented a shipboard meteorological observation in the Northwest of Indian Ocean. The third-part data are supported important for validating the satellite retrieved SST. In this study, the daily mean SST from the shipboard observation is obtained with some quality control processes. After imposing the temporal and spatial windows, we obtain a total 15 matching points of the daily mean TMI SST and 18 matching points for OSTIA.

After evaluating by the shipboard SST, the mean bias of the TMI SST is 1.79°C, and the root mean square error is 1.80°C. At the same time, the mean bias of the OSTIA SST is 0.73°C and the root mean square error is 0.99°C. These statistic analyses reveal the improvement of the merging SST than the satellite data retrieved only from the microwave.

We further discuss the possible factors affecting the errors of satellite SST. The results reveal that the wind speed and the air temperature are highly correlated with the TMI SST errors. The dependences of the TMI SST errors on the sight, the air pressure and the relative humidity are not significant. As far as the OSTIA SST is mentioned, the air temperature is the most important factor that is highly correlated with the SST error, and the dependence of the OSTIA SST error on the relative humidity is also significant.

Acknowledgements

The TMI data are produced by remote sensing systems and sponsored by the NASA Earth Sciences Program (www.remss.com), The OSTIA SST data are provided by the National Centre for Ocean Forecasting of UK (http://ghrsst-pp.metoffice.com), and the authors download the ETOPO-5min data from website http://www.ngdc.noaa.gov/.

References

Bell M M, Montgomery M T, Emanuel K A. 2012. Air-sea enthalpy and momentum exchange at major hurricane wind speeds observed during CBLAST. J Atmos Sci, 69: 3197–3222

Burkill P H, Mantoura R F C, Owens N J P. 1993. Biogeochemical cycling in the northwestern Indian Ocean: a brief overview. Deep-Sea Res 40(3): 643–649

Chen Dake, Lian Tao, Fu Congbin, et al. 2015. Strong influence of westerly wind bursts on El Niño diversity. Nat Geosci, 8: 339–345

Dong C M, Nencioli F, Liu Y, et al. 2011. An automated approach to detect oceanic eddies from satellite remotely sensed sea surface temperature data. IEEE Geoscience and Remote Sensing Letters, 8(6): 1055–1059

Donlon C J, Casey K S, Robinson I S, et al. 2009. The GODAE high-resolution sea surface temperature pilot project. Oceanography, 22: 34–45

Donlon C J, Martin M, Stark J, et al. 2012. The operational sea surface temperature and sea ice analysis (OSTIA) system. Remote Sensing of Environment, 116: 140–158

Donlon C J, Minnett P J, Gentemann C, et al. 2002. Toward improved validation of satellite sea surface skin temperature measurements for climate research. J Climate, 15: 353–369

Gentemann C L. 2014. Three way validation of MODIS and AMSR-E sea surface temperatures. J Geophys Res, 119: 2583–2598

Gentemann C L, Wentz F J, Mears C A, et al. 2004. In situ validation of tropical rainfall measuring mission microwave sea surface temperatures. Journal of Geophysical Research, 109: C04021

Hu Haibo, Hong Xiaoyuan, Zhang Yuan, et al. 2013. The critical role of Indian summer monsoon on the remote forcing between Indian and Northwest Pacific during El Niño decaying year. Sci China: Earth Sci, 56(3): 408–417

Lian Tao, Chen Dake, Tang Youmin, et al. 2014. Effects of westerly wind bursts on El Niño: a new perspective. Geophys Res Lett, 41(10): 3522–3527

Liu Xiaohui, Chen Dake, Dong Changming, et al. 2016. Variation of the Kuroshio intrusion pathways northeast of Taiwan using the Lagrangian method. Sci China: Earth Sci, 59: 268–280

Liu Xiaohui, Dong Changming, Chen Dake, et al. 2014. The pattern and variability of winter Kuroshio intrusion northeast of Taiwan. J Geophys Res, 119: 5380–5394

O'Carroll A G, August T, Le Borgne P, et al. 2012. The accuracy of SST retrievals from METOP-A IASI and AVHRR using the EUMETSAT OSI-SAF matchup dataset. Remote Sensing of Environment, 126: 184–194

O'Carroll A G, Eyre J R, Saunders R W. 2008. Three-way error analysis between AATSR, AMSR-E, and in situ sea surface temperature observations. J Atmos Oceanic Technol, 25(7): 1197–1207

Parekh A, Sharma R, Sarkar A. 2007. A comparative assessment of surface wind speed and sea surface temperature over the Indian Ocean by TMI, MSMR, and ERA-40. J Atmos Oceanic Technol, 24: 1131–1142

Park K A, Chung J Y, Kim K, et al. 1994. A study on comparison of satellite-tracked drifter temperature with satellite-derived sea surface temperature of NOAA/NESDIS. Korean J Remote Sens, 10(2): 83–107

Park K A, Chung J Y, Kim K, et al. 1999. Sea surface temperature retrievals optimized to the East Sea (Sea of Japan) using NOAA/AVHRR data. Marine Technology Society Journal, 33(1): 23–35

Park K A, Lee E Y, Chung S R, et al. 2011. Accuracy assessment of sea surface temperature from NOAA/AVHRR data in the seas around Korea and error characteristics. Korean J Remote Sens, 27(6): 663–675

Qiu C H, Wang D X, Kawamura H, et al. 2009. Validation of AVHRR and TMI-derived sea surface temperature in the northern South China Sea. Cont Shelf Res, 29(20): 2358–2366

Reynolds R W. 1993. Impact of mount Pinatubo aerosols on satellite-derived sea surface temperatures. J Climate, 6: 768–774

Reynolds R W, Gentemann C L, Corlett G K. 2010. Evaluation of AATSR and TMI satellite SST data. J Climate, 23(1): 152–165

Senan R, Anith S, Sengupta D. 2001. Validation of SST and WS from TRMM Using North Indian Ocean Moored Buoy Observations. CAOS Report 2001AS1, Centre for Atmospheric and Oceanic Sciences, Indian Institute of Science, Bangalore, Indian

Stark J D, Donlon C J, Martin M J, et al. 2007. OSTIA: an operational, high resolution, real time, global sea surface temperature analysis system. In OCEANS 2007. Marine challenges: coastline to deep sea. Aberdeen: IEEE Ocean Engineering Society, 331–334, doi: 10.1109/ OCEANSE. 2007. 4302251

Udaya B T V S, Rahman S H, Pavan I D, et al. 2009. Comparison of AMSR-E and TMI sea surface temperature with Argo near-surface temperature over the Indian Ocean. Int J Remote Sens, 30: 2669–2684

Walton C C. 1988. Nonlinear multichannel algorithms for estimating sea surface temperature with AVHRR satellite data. J Appl Meteor, 27: 115–124

Wentz F J, Gentemann C, Smith D, et al. 2000. Satellite measurements of sea surface temperature through clouds. Science, 288(5467): 847–850

Williams G N, Zaidman P C, Glembocki N G, et al. 2014. Comparison between remotely-sensed sea-surface temperature (AVHRR) and in situ records in San Matías Gulf (Patagonia, Argentina). Latin American Journal of Aquatic Research, 42(1): 192–203

Wu Qiaoyan, Yan Ying, Chen Dake. 2013. A linear Markov model for East Asian monsoon seasonal forecast. Journal of Climate, 26: 5183–5195

Wu Qiaoyan, Yan Ying, Chen Dake. 2016. Seasonal prediction of East Asian monsoon precipitation: skill sensitivity to various climate variabilities. Int J Climatol, 36: 324–333